

# A simple application of the Bailey–Orowan creep model to Fe–39.8 at % Al and $\gamma/\gamma' - \alpha$

J. D. WHITTENBERGER

NASA, Lewis Research Center, Cleveland, Ohio 44135, USA

R. V. KRISHNAN

National Aeronautical Laboratory, Bangalore 560017, India

A method which allows calculation of recovery rates and work hardening coefficients for creep from simple constant velocity compression experiments is described. Stressing rates and straining rates are computed from the measured load–time curves, and these quantities are then fitted to the universal form of the Bailey–Orowan equation for creep. The techniques were applied to B2 crystal structure Fe–39.8 at % Al intermetallics and the directionally solidified eutectic alloy  $\gamma/\gamma' - \alpha$  compression tested between 1200 and 1400 K. The recovery rates were found to be functions of nominal strain rate, stress, and temperature; the hardening coefficients were dependent only on temperature. Hardening coefficients for the aluminides are small ( $< 0.002$  of the elastic modulus) and are believed to be due to the lack of dislocation barriers. A more typical value for the hardening coefficient ( $\sim 0.05$  of the elastic modulus) was observed in  $\gamma/\gamma' - \alpha$ . Recovery rates and hardening coefficients can be described in terms of stress and temperature, and the equations used to estimate creep rates.

## 1. Introduction

The Bailey–Orowan creep model envisages high temperature deformation as a competition between recovery and hardening processes. In spite of this simplicity, the concept has not been widely utilized due to the difficulties associated with measurement of appropriate recovery rates and hardening coefficients. Recently Gan [1] has utilized a load variation method to evaluate the Bailey–Orowan model. Through small disruptions in load and variable straining rates during a nominally constant load tensile creep test, he was able simultaneously to measure the stressing and straining rates,  $d\sigma/dt = \dot{\sigma}$  and  $de/dt = \dot{\epsilon}$ , respectively. These values were then fitted to the more universal form of the Bailey–Orowan expression,

$$\dot{\sigma} = -r + h\dot{\epsilon} \quad (1)$$

where  $r$  is the recovery rate and  $h$  is the work hardening coefficient for creep. Thus Gan was able to determine both  $r$  and  $h$  from a single experiment.

Equation 1 can be used to determine the recovery rate and work hardening coefficients during both non-steady state and steady state conditions. In particular, evaluation of  $r$  and  $h$  from Equation 1 is simple and direct, if  $r$  and  $h$  are constant. This seems to be the case once some deformation has taken place, for Wilshire and co-workers [2, 3] have demonstrated that  $r$  and  $h$  are essentially constant after about 0.2 of the transient creep has been completed. Thus any method which allows independent evaluation of the stressing and straining rates during high temperature deformation should permit evaluation of the recovery rate and work hardening coefficient for creep.

Constant cross-head speed compression tests are currently being conducted at high temperatures to evaluate the slow plastic flow properties of experimental materials. To date the test information has been interpreted in terms of stress–strain and flow stress–strain rate behaviour [4, 5]; however it appears that the results of such con-

stant velocity tests contain sufficient data to allow computation of instantaneous stressing rates as well. Thus it could be possible to determine  $r$  and  $h$  by a much simpler experimental method than that proposed by Gan.

During plastic flow in compression under constant cross-head speed conditions, the gauge length  $l$  at any time  $t$  is given by

$$l = l_0 - Xt \quad (2)$$

where  $l_0$  is the original gauge length and  $X$  is the cross-head velocity. From the definition of true strain, it can be shown that

$$\dot{\epsilon} = -X/l. \quad (3)$$

Also from the definition of true stress and compressive test conditions

$$\sigma = -P/A. \quad (4)$$

Where  $\sigma$  is the true stress,  $P$  is the load and  $A$  is the instantaneous area. Differentiation of both sides of Equation 4 with respect to time yields

$$d\sigma/dt = \dot{\sigma} = (P/A^2)dA/dt - (1/A)dP/dt \quad (5)$$

which in turn can be reduced to

$$\dot{\sigma} = \sigma(X/l) - (1/A)dP/dt \quad (6)$$

by use of Equation 2 and the conservation of volume principle. Equations 6 and 3, when combined with Equation 1, will permit  $r$  and  $h$  to be calculated from preset and readily measurable (computed) quantities.

The following presents the results of a study to determine the recovery rates and work hardening coefficients for creep from constant cross-head speed compressive tests. This analysis was applied to the load-time-deformation data from several B2 crystal structure Fe-39.8 Al intermetallic materials where  $r$  and  $h$  were calculated as functions of temperature, stress, strain rate and processing conditions. Fe-39.8 Al is one of several B2 aluminides currently being examined at the Lewis Research Center for potential use as high temperature structural materials. Due to the unusually low work hardening coefficients computed for these aluminides, the analysis was also applied to appropriate test data for the directionally solidified eutectic (d.s.e) alloy  $\gamma/\gamma'-\alpha$ .

## 2. Experimental procedures

Constant cross-head speed compression tests have been conducted in a universal testing machine on

nominally 5 mm diameter, 10 mm long right cylindrical specimens. These tests were undertaken in air between 1200 and 1400 K at speeds ranging from  $2.12 \times 10^{-2}$  to  $2.12 \times 10^{-6}$  mm sec<sup>-1</sup>. During testing the load was autographically recorded as a function of time, and both stress and strain data calculated from such load-time charts. True stresses were computed on the basis of conservation of volume while strains were determined either by the offset method [6] when an elastic region could be discerned or by cross-head displacement when little elastic deformation could be seen. In general the calculated strain at the end of a test agreed well ( $\pm 10\%$  of the total strain) with that determined by the measured change in length; however, for consistency, all calculated strains were normalized to the actual change in length. Further details concerning the test procedures are given in [4].

The majority of the calculations are based on the compression test results for Fe-39.8 at % Al. This particular B2 crystal structure iron aluminide was produced by 1200 K extrusion of pre-alloyed powders. Tests were conducted on both as-extruded stock as well as material which has been heat treated for 16 h at 1300 K. Both of these forms are polycrystalline and possess a grain size of about 10  $\mu$ m diameter which was maintained even after testing to  $-0.1$  or more strain at either 1200 or 1300 K. Some grain growth to about 20  $\mu$ m, however, was observed after testing at 1400 K. Other details about this intermetallic can be found in [4].

A few calculations were also carried out on compressive test data for a  $\gamma/\gamma'-\alpha$  directionally solidified eutectic alloy. This material was grown at 17 mm h<sup>-1</sup> by a modified Bridgeman technique from pre-alloyed stock of nominal composition (wt %): Ni-32.3 Mo-6.3 Al. The microstructure consisted of essentially infinitely long, square cross-section (about 0.5  $\mu$ m on edge) Mo fibres in a  $\gamma$  (Ni solid solution) plus  $\gamma'$  (Ni<sub>3</sub>Al) matrix where the fibre length was parallel to the growth direction. More particulars about  $\gamma/\gamma'-\alpha$  are given in [7]. Compression tests at 1273 K with stressing direction parallel to the fibre axis were conducted on three different material conditions: as-grown, annealed 1 h at 1023 K, and hot swaged 25% at 1023 K. The latter thermomechanical processing was undertaken in an effort to improve the high temperature creep strength [5].

While the instantaneous strain rates could be

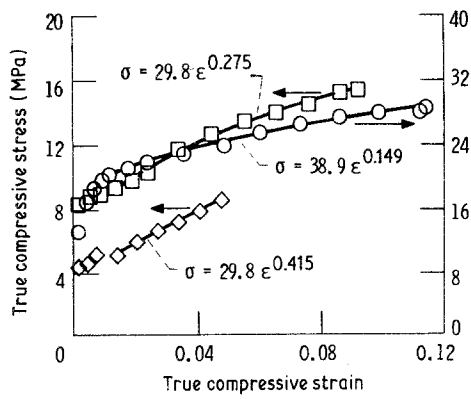


Figure 1 Typical true compressive stress-strain diagrams as a function of cross-head velocity for as-extruded Fe-39.8 at % Al tested at 1200 K. The cross-head velocities shown are:  $\circ 2.12 \times 10^{-4} \text{ mm sec}^{-1}$ ;  $\square 2.12 \times 10^{-5} \text{ mm sec}^{-1}$ ;  $\diamond 2.12 \times 10^{-6} \text{ mm sec}^{-1}$ .

directly computed from Equation 3, calculation of instantaneous stressing rates could not be made as easily. Instead  $dP/dt$  had to be initially determined by linear regression techniques, and this value inserted into Equation 6. The resultant  $\dot{\sigma}$ ,  $\dot{\epsilon}$  data were then fitted to Equation 1 by regression methods

and  $r$ ,  $h$  determined. In general the regression coefficients,  $R^2$ , for such fits were  $\geq 0.95$ .

### 3. Results

Typical stress-strain diagrams for as-extruded Fe-39.8 at % Al are shown in Fig. 1. This behaviour is representative of both as-extruded and heat-treated aluminides tested between 1200 and 1400 K in that continuous strain hardening is observed for all velocities. Two examples of load-time curves used to determine  $dP/dt$ , and the calculated stressing rate-straining rate behaviour are presented in Fig. 2. Parts (a) and (c) illustrate that load can be well represented as a linear function of time over the majority of the test. Thus  $dP/dt$  is a constant and evaluation of  $\dot{\sigma}$  from Equation 6 is straightforward. The stressing rate-straining rate data (Figs. 2b and d) also exhibit linear behaviour; hence recovery rates and work hardening coefficients for creep could be readily calculated. These are shown in Fig. 3 as functions of nominal strain rate (half the sum of the initial and final strain rates; about 0.95 the initial rate), temperature and heat-treatment condition.

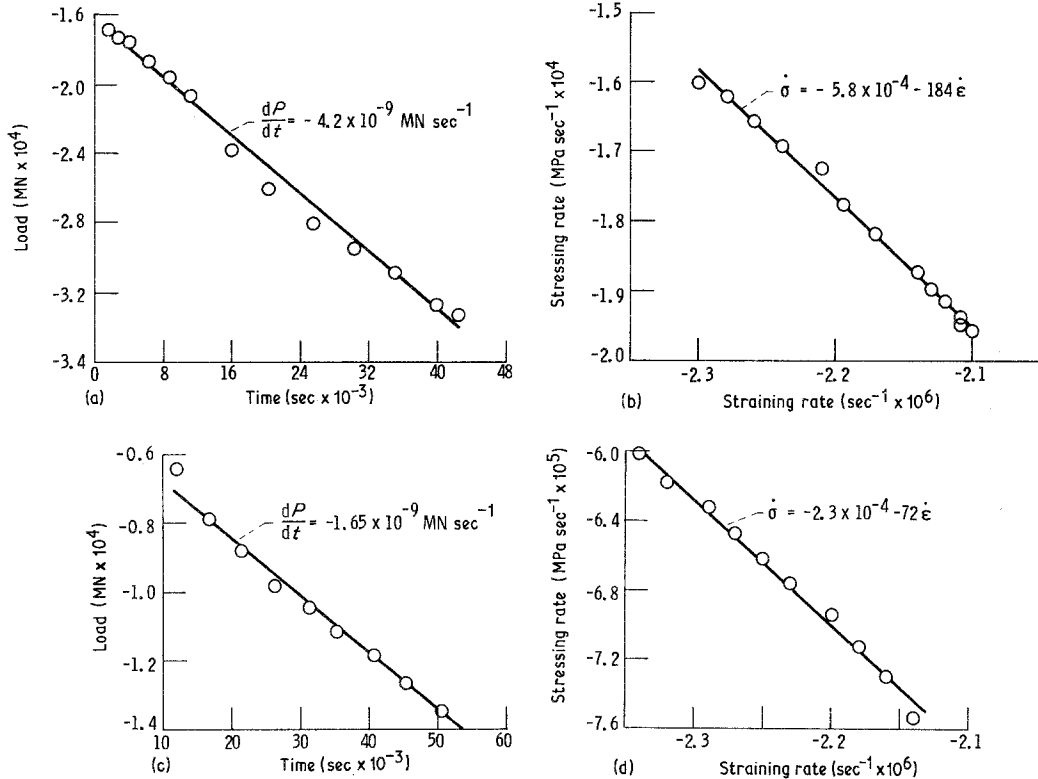


Figure 2 Typical load-time curves ((a) and (c)) and stressing rate-straining rate curves ((b) and (d)) for as-extruded Fe-39.8 at % Al tested at a constant velocity of  $2.12 \times 10^{-5} \text{ mm sec}^{-1}$  at 1200 K ((a) and (b)) and 1300 K ((c) and (d)). Regression coefficients of all fits  $\geq 0.99$ .

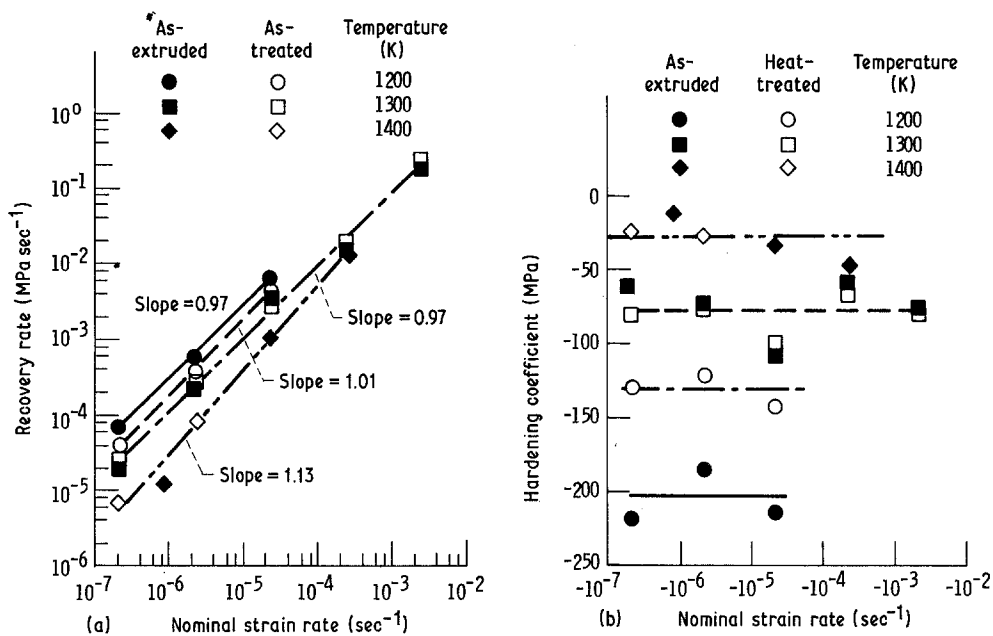


Figure 3 Recovery rates (a) and work hardening coefficients for creep (b) as functions of nominal strain rate and temperature for Fe-39.8 at % Al materials. Regression coefficients for (a)  $\geq 0.98$ . Horizontal lines in (b) represent average values.

The recovery rate–nominal strain rate data in Fig. 3a illustrate that these quantities are dependent on the temperature. In addition they are directly proportional to each other, since the slope of the log–log plots is essentially unity for all conditions. Statistical testing (dummy variable coupled with “*F*”-test) of the data in Fig. 3a demonstrated that the as-extruded and heat-treated Fe-39.8 at % Al intermetallics possessed different recovery rate–strain rate behaviour at 1200 K; however at 1300 and 1400 K both materials exhibited similar characteristics.

While recovery rate is dependent on strain rate, the work hardening coefficient for creep is apparently independent, since no trends in  $h$ – $\dot{\epsilon}$  behaviour are visible in Fig. 3b. On the other hand, the hardening coefficients do depend on temperature and heat treatment. Statistical testing confirmed that at 1200 K the  $h$  for the as-extruded Fe-39.8 at % Al is indeed slightly more negative than that for the heat-treated material; however no differences in hardening coefficients were found at the higher test temperatures.

Since the hardening coefficients shown in Fig. 3b seemed rather low, compression test data for the d.s.e. alloy  $\gamma/\gamma'$ – $\alpha$  were examined to determine if the method of analysis was at fault. Typical stress–strain diagrams for as-grown and thermomechanically processed  $\gamma/\gamma'$ – $\alpha$  are shown

in Fig. 4. The behaviour of this alloy is somewhat different from that of the aluminides (Fig. 1) where  $\gamma/\gamma'$ – $\alpha$  undergoes only a small amount of strain hardening before reaching a more or less constant flow stress at  $\sim 1\%$  strain. Examples of a load–time curve and the resultant stressing rate–straining rate behaviour are given in Fig. 5. As was the case for Fe-39.8 at % Al (Fig. 2),  $dP/dt$  is essentially constant and  $\dot{\sigma}$ – $\dot{\epsilon}$  demonstrates a linear relationship.

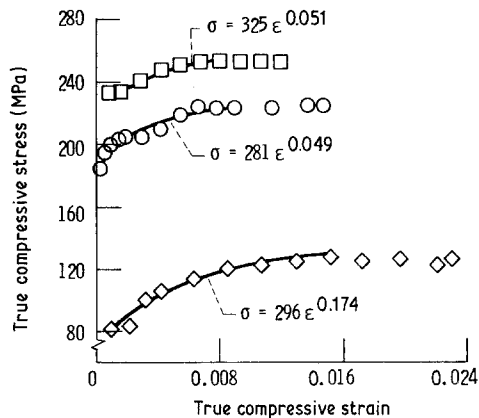


Figure 4 Typical true compressive stress–strain diagrams for as-grown and thermomechanically processed  $\gamma/\gamma'$ – $\alpha$  tested at a constant rate of  $2.12 \times 10^{-6} \text{ mm sec}^{-1}$  at 1273 K.  $\circ$  as-grown;  $\square$  annealed 1 h at 1023 K;  $\diamond$  swaged 25% at 1023 K.

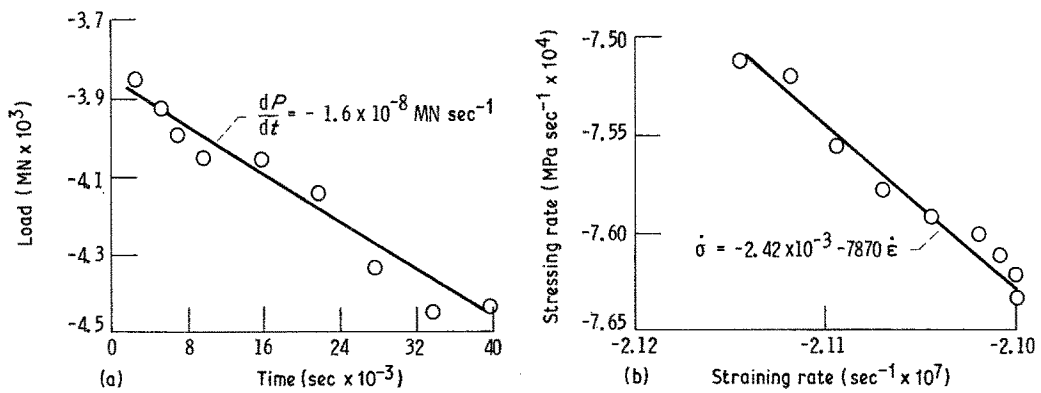


Figure 5 The load–time (a) and stressing rate–straining rate (b) curves for as-grown  $\gamma/\gamma'$ - $\alpha$  tested at a constant velocity of  $2.12 \times 10^{-6}$  mm sec $^{-1}$  at 1273 K. All regression coefficients  $\geq 0.95$ .

The results of the recovery rate, work hardening coefficient for creep calculations as functions of nominal strain rate and processing are shown in Fig. 6. The behaviour of  $\gamma/\gamma'$ - $\alpha$  is similar to that for the intermetallics (Fig. 3) where the recovery rate is directly proportional to the strain rate while the hardening coefficient is independent of the strain rate. Statistical testing of these data reveal that: 1.  $r$  and  $h$  for the as-grown and annealed 1 h at 1023 K materials could not be distinguished from one another; and 2. that swaging did significantly affect both  $r$  and  $h$  in comparison to the other processing techniques.

#### 4. Discussion

The general behaviour of the recovery rates and work hardening coefficients for creep calculated from Equation 1 and constant cross-head speed

compression test data is quite similar to that previously observed. For example, a linear dependency between recovery rate and strain rate (Figs. 3a and 6a) and constant work hardening coefficients (Figs. 3b and 6b) have been found by Wilshire and co-workers [2, 3, 8]. Due to the direct proportionality between  $\dot{\epsilon}$  and  $r$ , the observation that the recovery rate for Fe-39.8 at% Al depends on test temperature is not surprising. Additionally the increase in hardening coefficient (decrease in absolute magnitude) with higher testing temperature for the intermetallics is expected, because the strength decreases as temperature is increased [4].

The most puzzling result of the current study is the very low hardening coefficients for creep in the intermetallics (Fig. 3b). Based on interpolation, the elastic modulus for Fe-39.8 at% Al [9]

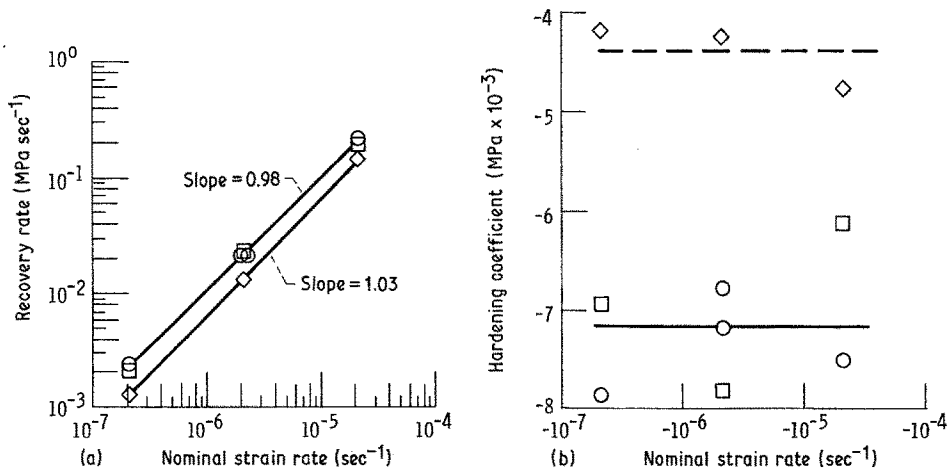


Figure 6 Recovery rates (a) and work hardening coefficients for creep (b) as a function of nominal strain rate for  $\gamma/\gamma'$ - $\alpha$  tested at 1273 K. Regression coefficients for (a)  $\geq 0.95$ . Horizontal lines in (b) represent average values.  $\circ$  as-grown;  $\square$  heat-treated 1 h at 1023 K;  $\diamond$  swaged 25% at 1023 K.

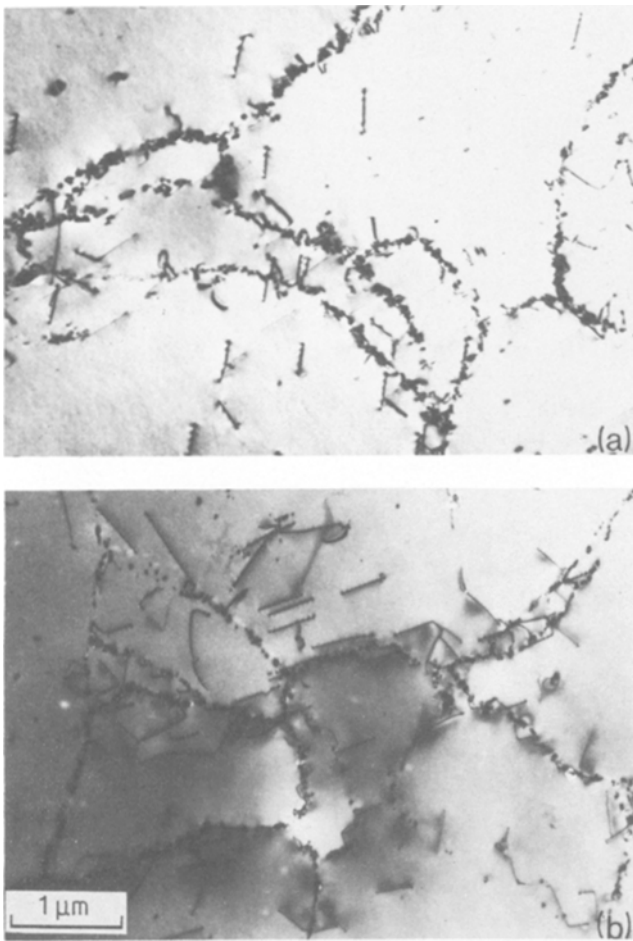


Figure 7 Transmission electron photomicrographs of as-extruded Fe-39.8 at % Al tested at (a) 1200 K and (b) 1300 K at a nominal strain rate of  $2 \times 10^{-5} \text{ mm sec}^{-1}$  to  $-0.1$  strain.

is about 93 GPa at 1200 K; thus the work hardening coefficient for creep in either material at 1200 K is about 0.0015 of the modulus. In general other studies [10, 11] of  $h$ 's shown that they lie between  $0.05 E$  and  $E$ , where  $E$  is the elastic modulus at temperature. While values of  $h \geq 0.25 E$  have been criticized [12, 13] as being unrealistically high, perhaps owing to the experimental/calculation methods, measurements of  $h < 0.01 E$  have not been reported.

Because the possibility existed that the low work hardening coefficients for creep in the Fe-39.8 at % Al materials could have been due to the method of calculation,  $h$ 's were determined for  $\gamma/\gamma' - \alpha$  (Fig. 6b). The average value for the combined as-grown and annealed 1 h at 1023 K data is  $-7.2 \text{ GPa}$ , which can be compared with the elastic modulus of  $\sim 138 \text{ GPa}$  measured for a d.s.e.  $\gamma/\gamma' - \alpha$  containing nominally 5.9 wt % Al-29.7 wt % Mo-1.65 wt % V-1.2 wt % Re-balance Ni [14]. This comparison yields a  $|h/E|$  ratio of about 0.05, which is reasonable. Thus the calcu-

lation method is not directly responsible for the low hardening coefficients for creep in the aluminides.

Evans and Knowles [15] have proposed a model which can account for a low work hardening coefficient for creep in a material which undergoes recovery controlled deformation. Through dislocation glide and climb processes, a three-dimensional network is established, and the maintenance of this dislocation network is responsible for creep. In their development Evans and Knowles predict that

$$h = \alpha \mu / 2s\rho^{0.5} \quad (7)$$

where  $\alpha$  is a constant of the order of one,  $\mu$  is the shear modulus,  $s$  is an average slip distance, and  $\rho$  is the dislocation density. If  $s$  is large, then Equation 7 would predict a low work hardening coefficient for creep. This seems to be the case for the Fe-39.8 at % Al materials, as very few barriers to dislocation motion are found even in specimens tested to large strains at relatively high velocities (Fig. 7).

Fig. 7 shows transmission electron photomicrographs of as-extruded specimens tested at 1200 and 1300 K. Sections for transmission electron microscopy were taken perpendicular to the stress axis and prepared with a 5% perchloric acid in ethanol solution at 273 K and 20 volts d.c. The photomicrographs reveal that there are no subgrains formed in the material during deformation and few, if any, dislocation pile-ups were seen even at grain boundaries. In addition the network of oxide particles present in the Fe-39.8 at % Al materials extruded at 1200 K do not appear to act as dislocation barriers. The behaviour of the heat-treated aluminide was identical to that of the as-extruded material.

With regards to overall mechanical behaviour, the trends of the recovery rates and work hardening coefficients for the aluminides and  $\gamma/\gamma'-\alpha$  are in general agreement with previously reported results. Analysis [4] of the flow stress-strain and flow stress-strain rate data for the two Fe-39.8 at % Al materials revealed that their characteristics were nearly identical between 1200 and 1400 K. The recovery rate, hardening coefficient data for the intermetallics (Fig. 3) indicate that these quantities are similar for both materials at 1300 and 1400 K. However, these data reveal that there is a difference in performance at 1200 K where the as-extruded form possesses both higher recovery rates and a more negative hardening coefficient than the heat-treated stock. While the  $r$ ,  $h$  calculations for  $\gamma/\gamma'-\alpha$  (Fig. 6) could detect the known difference between and swaged and unworked materials [5], the recovery rates and hardening coefficients did not reflect the lower strength of the as-grown material in comparison to the annealed material (Fig. 4). This discrepancy should, however, be tempered by the observation that no statistical difference could be discerned between the flow stress-strain rate characteristics for these processing conditions [5].

While a knowledge of the recovery rates and hardening coefficient can be used to calculate steady state creep rates via the Bailey-Orowan equation

$$\dot{\epsilon}_{ss} = r/h \quad (8)$$

this equation cannot be directly applied in a predictive manner unless  $r$  and  $h$  are related to common, controllable parameters. Since recovery rates are almost directly proportional to the nominal strain rate (Figs. 3a and 6a), an equation of the form

$$\hat{r} \propto \sigma^n \exp(-Q/RT) \quad (9)$$

was used where  $\hat{r}$  is the estimated recovery rate,  $n$  is a stress exponent,  $Q$  is an activation energy, and  $R$ ,  $T$  have their usual meanings.

For  $\gamma/\gamma'-\alpha$  the stress value to be inserted into Equation 8 should clearly be the more or less constant flow stresses (Fig. 4 and [5]). The choice for the aluminides is not as straightforward, because the stress-strain diagrams show continuous work hardening (Fig. 1 and [4]). To be consistent with [4], the flow stresses at the end of testing were used for Fe-39.8 at % Al. In reality any stress level taken after  $\sim 3\%$  deformation would be sufficient, since the work hardening is slight beyond this point.

For as-grown and annealed  $\gamma/\gamma'-\alpha$  at 1273 K,

$$\hat{r} = 9.33 \times 10^{-24} \sigma^{8.6} \quad (10)$$

where the standard deviation on  $n = 1.1$ , and the regression coefficient was 0.92. The fit of the combined aluminide data yielded

$$\hat{r} = 1.6 \times 10^8 \sigma^{3.33} \exp(-356/RT) \quad (11)$$

with the regression coefficient = 0.98, standard deviation on  $n = 0.11$  and  $Q = 24$  kJ.

The hardening coefficient data for the aluminides (Fig. 3b) demonstrate that they are dependent on test temperature but not on strain rate. Additionally plots and analysis of  $h-\sigma$  data revealed, as expected, that hardening coefficients were not a function of stress. To obtain a single equation, the  $h$  values were averaged and fitted as an inverse function of temperature:

$$\hat{h} = 828 - 1190000/T \quad (12)$$

where  $\hat{h}$  is the estimated hardening coefficient and the regression coefficient is 0.98.

The predictive Equations 11 and 12 plus Equation 10 with the average hardening coefficient ( $-7165$  MPa) for unworked  $\gamma/\gamma'-\alpha$  can be substituted into Equation 8, and steady state creep rates estimated. In Fig. 8 the ratio of the nominal test strain rate divided by  $\hat{r}/\hat{h}$  is shown as functions of temperature and stress. For both materials the predicted strain rates lie within a factor of  $\sim 2$  of the nominal rate, and the predicted steady state values are generally greater than the actual rates. While the comparison for Fe-39.8 at % Al is not strictly correct since steady state was not achieved, the behaviour of both the aluminide and d.s.e. alloy is quite similar. Therefore recovery rate and

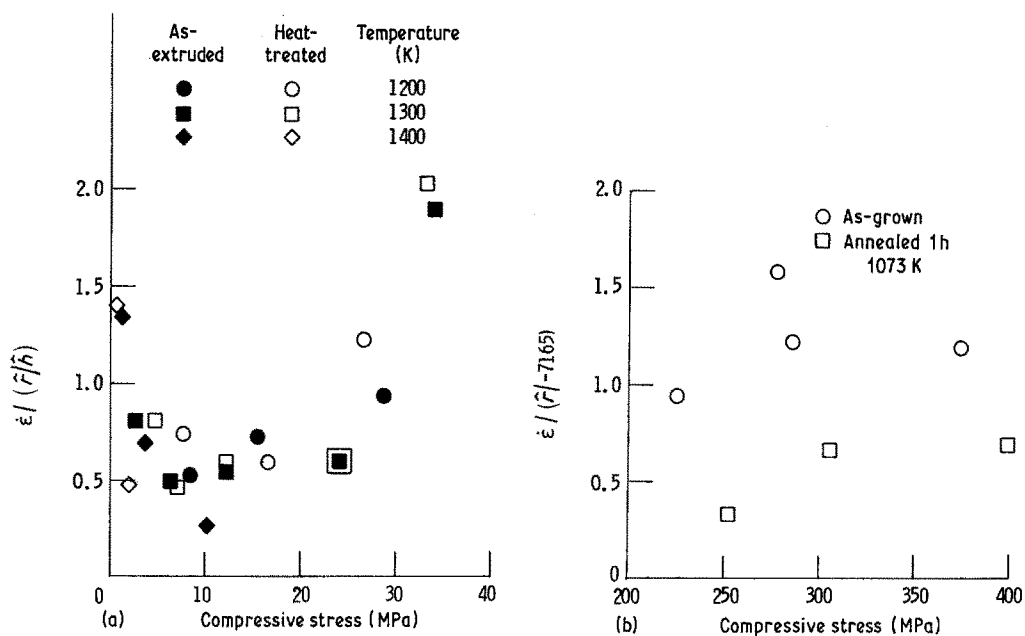


Figure 8 Ratio of nominal strain rate to  $\dot{\epsilon}/\dot{\epsilon}_s$  as functions of temperature and stress for Fe-39.8 at % Al (a) and  $\gamma/\gamma'-\alpha$  (b).

hardening coefficient equations could prove useful as a means to forecast creep rates.

The constant cross-head speed compression test method outlined in this paper is capable of determining both recovery rates and hardening coefficients for creep from a relatively simple experiment. This approach is based on stressing rate and straining rate data which are then fitted to the universal form of the Bailey-Orowan equation for creep. In practice it was found that this technique could be generally implemented on stress-strain data which can be described by the Ludwik-Hollomon equation [16]

$$\sigma = K\epsilon^m, \quad (13)$$

where  $K$  is a constant and  $m$  is a strain hardening coefficient. Typical examples of valid ranges of data and appropriate equations are illustrated in Figs. 1 and 4. Finally it should be noted that the methodology could be adapted to tensile testing; however one must be certain that the deformation occurs within the gauge section.

## 5. Conclusions

Based on an analysis of load-time curves for two different materials, it is concluded that constant velocity compression test data can be fitted to the universal form of the Bailey-Orowan equation for creep, and the recovery rates and work harden-

ing coefficients for creep calculated. Application of this method to the B2 crystal structure intermetallic Fe-39.8 at % Al and the d.s.e. alloy  $\gamma/\gamma'-\alpha$  yielded recovery rates which were dependent on strain rate, stress and temperature. While the work hardening coefficient for  $\gamma/\gamma'-\alpha$  was about 0.05 of the elastic modulus, the work hardening coefficients for Fe-39.8 at % Al were less than 0.002 of the modulus.

## Acknowledgements

One of the authors (RVK) thanks the National Research Council for the award of a Research Associateship, the Lewis Research Center for providing the laboratory facilities and the National Aeronautical Laboratory, Bangalore, India for granting leave to pursue this associateship programme. In addition both authors would like to acknowledge the many discussions and comments given by Michael V. Nathal.

## References

1. DERSHIN GAN, *J. Mater. Sci.* **17** (1982) 89.
2. D. SIDEY and B. WILSHIRE, *Met. Sci. J.* **3** (1969) 56.
3. J. M. BIRCH and B. WILSHIRE, *J. Mater. Sci.* **9** (1974) 871.
4. J. D. WHITTENBERGER, *J. Mater. Sci. Eng.* **57** (1983) 77.
5. J. D. WHITTENBERGER and G. WIRTH, *J. Mater.*



- Sci.* 18 (1983) 2581.
6. J. D. WHITTENBERGER, *Metall. Trans. A* 10A (1979) 1285.
  7. J. D. WHITTENBERGER and G. WIRTH, *Met. Sci.* 16 (1982) 383.
  8. P. L. THREADGILL and B. WILSHIRE, in "Creep Strength in Steel and High Temperature Alloys" (Metal Society, London, 1974).
  9. W. KOESTER and T. GOEDECHE, *Z. Metallkde.* 73 (1982) 111.
  10. G. J. LLOYD and R. J. McELROY, *Acta Metall.* 22 (1974) 339.
  11. W. J. EVANS, *Met. Sci.* 10 (1976) 170.
  12. C. R. BARRETT, C. N. AHLQUIST and W. D. NIX, *ibid.* 4 (1970) 41.
  13. S. TAKEUCHI and A. S. ARGON, *J. Mater. Sci.* 11 (1976) 1542.
  14. M. F. HENRY, M. R. JACKSON, M. F. X. GIGLIOTTI and P. B. NELSON, NASA CR-159416 (1979).
  15. H. E. EVANS and G. KNOWLES, in "Creep and Fracture of Engineering Materials and Structures", edited by B. Wilshire and D. R. J. Owen (Pineridge Press, Swansea, 1982).
  16. J. H. HOLLOMON, *Trans AIME* 162 (1945) 268.

*Received 9 March  
and accepted 6 June 1983*